

Selective growth of nanometre scale structures with high resolution using thermal energy in AFM lithography

This article has been downloaded from IOPscience. Please scroll down to see the full text article.

2005 Nanotechnology 16 3137

(<http://iopscience.iop.org/0957-4484/16/12/068>)

View [the table of contents for this issue](#), or go to the [journal homepage](#) for more

Download details:

IP Address: 115.145.196.108

The article was downloaded on 29/05/2013 at 14:04

Please note that [terms and conditions apply](#).

Selective growth of nanometre scale structures with high resolution using thermal energy in AFM lithography

Sunwoo Lee^{1,2}, Haiwon Lee^{1,2,4}, Byung-jae Park³ and Geun Young Yeom³

¹ Department of Chemistry, Hanyang University, Seoul 133-791, Korea

² The National Program for Tera-Level Nanodevices, Seoul 136-791, Korea

³ Department of Material Science and Engineering, Sungkunkwan University, Suwon 440-746, Korea

E-mail: haiwon@hanyang.ac.kr

Received 14 July 2005, in final form 4 October 2005

Published 11 November 2005

Online at stacks.iop.org/Nano/16/3137

Abstract

We report the effect of applied thermal energy in the fabrication of protruded nanostructures on tantalum (Ta) thin films using atomic force microscope (AFM) lithography and the fabrication of nanopatterns of Ta thin films by a dry etching process of protruded tantalum oxide (Ta₂O₅). Oxidized nanostructures with a high aspect ratio were successfully fabricated at high temperature by applying thermal energy. The lithographic speed of fabrication of protruded nanostructures was dramatically improved by the enhancement of electron transfer depending on the applied thermal energy and directional diffusion of OH⁻ ions depending on the increase of temperature. Nanopatterns of Ta with a high angle slope (over 80°) were fabricated by selective dry etching of Ta₂O₅.

(Some figures in this article are in colour only in the electronic version)

1. Introduction

Recently, an ArF excimer laser with 193 nm wavelength radiation has been used for patterning of nanoscale devices. However, on scaling down device dimensions to the nanometre range, optical lithography cannot pattern features 65 nm or smaller. There has been growing interest in fabricating structures whose critical dimensions lie in the sub-65 nm range for ultra-large scale integration (ULSI) circuit technology. In order to fabricate nanostructures with high spatial resolution, there have been many studies in next generation lithography (NGL) such as extreme ultraviolet radiation lithography (EUVL) [1–3], electron projection lithography (EPL) [4], soft x-ray lithography, nanoimprint lithography (NIL) [5], electrostatic nanolithography [6] and atomic force microscope (AFM) lithography [7–10]. Among these next generation lithography techniques, AFM lithography has been proven in

the selective growth of oxide layers with high aspect ratios and feature sizes below 50 nm, and can be successfully used for fabrication of vertical structures with feature sizes of a few nanometres. Advanced technologies are required to fabricate nanostructures which meet the previously mentioned requirements (feature size below 50 nm and high aspect ratio). The majority of local oxidation experiments have used a water column that is formed between an AFM tip and a substrate. Sugimura *et al* [7] reported on the electrochemical reactions between an AFM tip and a substrate. It was suggested that nanostructures are fabricated by the reaction between the decomposed electrons, OH⁻ ions and the substrate by the application of an external voltage ($\text{Si} + 2\text{OH}^- - 4\text{e}^- \rightarrow \text{SiO}_2 + 2\text{H}^+$). The line width and height of nanostructures generally increases as the tip bias increases [11, 12, 15]. The enhancement of the vertical growth rate of local oxidation on semiconductors has been reported by others. The fabrication method of oxidized nanostructures by reducing the space charge effect using an applied AC bias voltage between a tip and a substrate was successfully demonstrated by Dagata *et al*

⁴ Address for correspondence: Department of Chemistry, Hanyang University, 17 Haengdang-dong, Sungdong-gu, Seoul 133-791, Korea.

[13]. The fabrication method that makes use of ethyl alcohol liquid bridges as a source of oxyanion ions was suggested by Garcia *et al* [14].

The current work is designed to fabricate nanostructures with a high aspect ratio and narrow feature size under conditions of low humidity and elevated temperature by the emission of thermal energy. Prior to the simultaneous variation of temperature and humidity, Avouris *et al* [15] reported that the line width of nanostructures is certainly increased with increasing humidity at a constant temperature. Specifically, we investigated how AFM lithographic patterns are affected by the addition of thermal energy and the fabrication of tantalum nanopatterns by selective dry etching.

2. Experimental details

A heating system that isolates the thermal transmission with the external ambient environment was made to enhance the effect of thermal energy during AFM anodization lithography. The two experimental factors of humidity and temperature are controlled by the emission of thermal energy. After removing the humidity from the air inlet of the system, thermal energy and water vapour are introduced into the system. A Ta thin film was used as a substrate instead of tantalum nitride (TaN), tungsten (W), titanium (Ti), or chromium (Cr) thin films [16, 17] because Ta thin films form a high aspect ratio related to the work function and have low roughness and moderate electrical and thermal conductivities. After rinsing with acetone, Ta was deposited on an n-type Si(100) wafer ($\rho \sim 14\text{--}23 \text{ } \Omega \text{ cm}$, LG Siltron, Korea) by a magnetron sputtering system (CSS12, Chungsong, Korea) in the conditions of 100 W DC bias power and 5 mTorr working pressure. The thickness and roughness of the Ta thin film were ~ 10 and 0.06 nm, respectively. An Autoprobe CP (Park Scientific Instruments, USA) was used in the lithographic and imaging processes. The imaging process also used an XE-100 (Advanced Scanning Microscope, Korea) and both processes utilized a platinum-coated tip (CSC12/Pt, MicroMash, USA) in contact mode. Subsequently, protruded Ta₂O₅, which was fabricated by AFM lithography, was directly etched without a shadow mask by C₄F₈ gas using a magnetically enhanced inductively coupled plasma (MEICP) etching system.

3. Results and discussions

As shown in figure 1(a), it was found that the height of the Ta₂O₅ nanostructures was dramatically increased from 5 nm to about 20 nm in proportion to the external temperature change from 25 to 31 °C under the condition of a bias voltage of 22 V, a lithographic speed of 0.5 $\mu\text{m s}^{-1}$, and a constant humidity of 40%. Protruding Ta₂O₅ nanostructures fabricated under the condition of a bias voltage of 18 V and a lithographic speed of 1 $\mu\text{m s}^{-1}$, the optimized value for a high aspect ratio, are shown in figures 1(b) and (c). The ambient temperature and relative humidity were varied from 22 to 31 °C and from 41% to 30%, respectively. The line height of the nanostructures dramatically increased from 1–2 nm to 12–16 nm. However, the full width at half maximum (FWHM) of these nanostructures only moderately increased from 50 to 78 nm. Based on these results, it is suggested that lithographic oxidation is sensitive to the

temperature parameter dependence on the emission of thermal energy.

The film growth rate was explained according to the temperature variation in Grove's model [18]. According to Grove's model, at low temperatures the growth rate is limited by the chemical surface reaction. At high temperatures, however, the growth rate is limited by the mass transfer of gas molecules across the boundary layer. Grove therefore proposed that the growth rate is dramatically increased at high temperatures. Thus, at the elevated temperature in this system, where the mass transfer of gas molecules (OH⁻ ions dissociated by the electric field) from the tip to the substrate is very high, the electrochemical reactions between the substrate and the OH⁻ ions are very strongly activated. Consequently, the height of the protruded tantalum oxide nanopattern increases because of the reactions of OH⁻ ions at the local surface.

For different ambient temperatures, the water meniscus is shown in figure 2. At low humidity under room temperature (figure 2(a)), the electric field generated by an applied bias voltage forms the sharp water meniscus, which is the source of OH⁻ ions. Nanostructures with a sharp FWHM can be fabricated under these conditions, while at high humidity and room temperature (figure 2(b)) the electric field makes a wider water meniscus and wider nanostructures are fabricated. However, in the condition of a sharp water meniscus (figure 2(c)) formed at low humidity and elevated temperature, the diffusivity as well as the direction of diffusion of OH⁻ ions from the tip (anode) to the substrate (cathode) by the electric field is enhanced onto the local area of surface defined by the sharp meniscus. The concentration gradient of OH⁻ ions which migrate to the surface (the increase of OH⁻ ion concentration which can react on the substrate) is also increased in proportion to the improvement in diffusivity of OH⁻ ions at an elevated temperature.

In electrical characteristics, free electrons, which are excited by the collision of accelerated electrons toward a positive sample bias, act as a means of thermal transmission. These free electrons are more activated by the additionally applied thermal energy and the electron transfer between a substrate and a tip can be significantly enhanced by application of thermal energy. As a result of this phenomenon, the enhancement of free electron transfer played a central role in lowering the threshold voltage from 12 to 8 V (this work), which is an important factor in AFM lithography. The height of protruded nanostructures fabricated at 31 °C was higher than that of oxidized nanostructures fabricated at 22 °C due to the lower threshold voltage and enhanced diffusivity [18] of OH⁻ ions from the application of thermal energy and the increase of temperature. Thus, the growth of Ta₂O₅, which has a low threshold voltage at an elevated temperature, is induced in the local area because of the sharp water meniscus, directional diffusion, and the increase in concentration of OH⁻ ions, which can react with the substrate.

Nanostructures oxidized at the high speed of 300–400 $\mu\text{m s}^{-1}$, a bias voltage of 18 V, an elevated temperature of 31 °C and a low humidity of 30% are shown in figure 3. As the lithographic speed increases from 300 to 400 $\mu\text{m s}^{-1}$, the nanostructure height decreases from 2.5 to 1.7 nm, and the FWHM of nanostructures decreases from 60 to 38 nm.

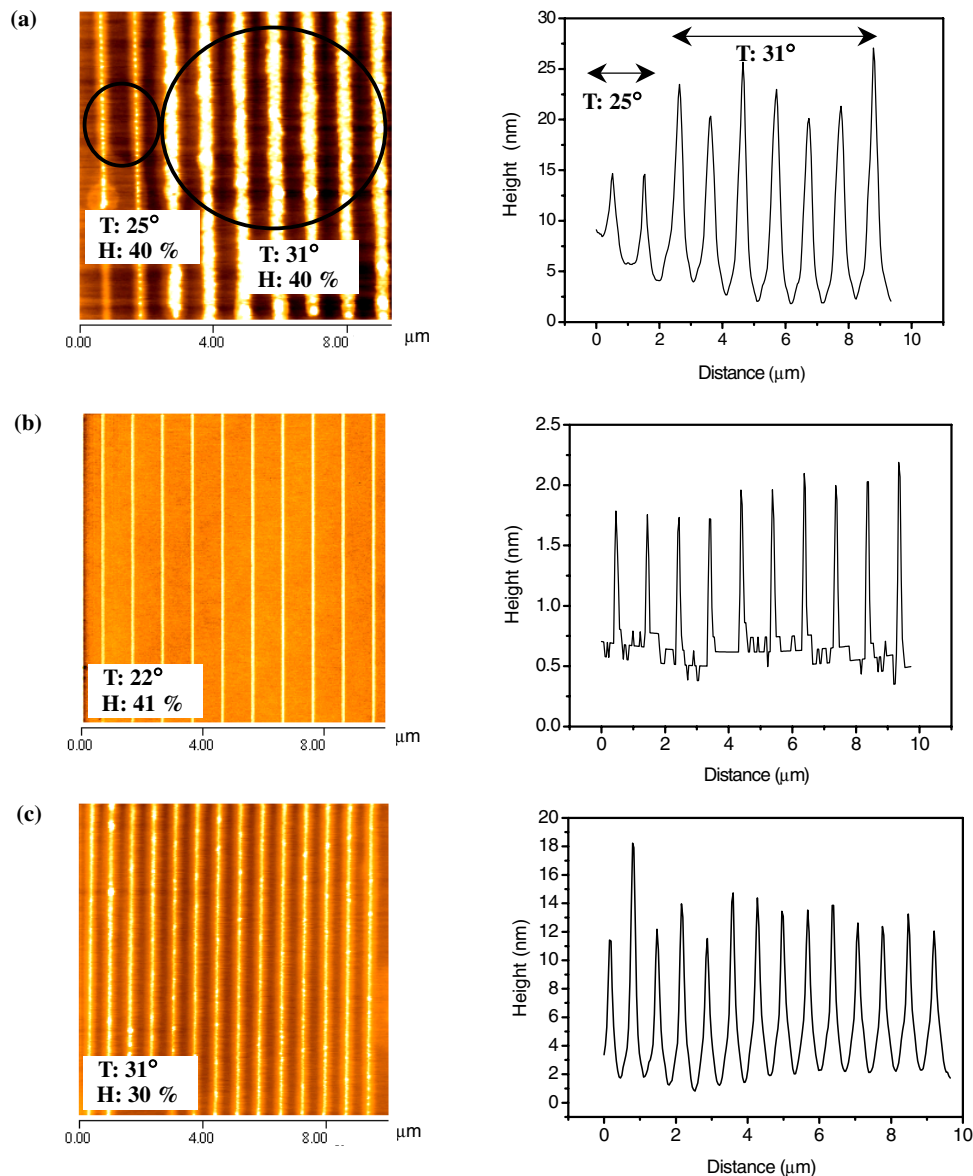


Figure 1. AFM images of Ta_2O_5 nanostructures fabricated at varying temperatures and humidities. (a) Oxidized nanostructures fabricated at different temperatures (25 and 31 °C, from left to right) and constant humidity of 40%, (b) nanostructures fabricated at a temperature of 22 °C and a high humidity of 41%, and (c) nanostructures fabricated at an elevated temperature of 31 °C and a low humidity of 30%.

However, nanostructures of Ta_2O_5 were not fabricated at lithographic speeds above $10 \mu\text{m s}^{-1}$ with a humidity of 41% and a temperature of 22 °C. It was thought that nanostructures could be fabricated at high lithographic speeds because of the electrochemical reaction by enhanced diffusivity of OH^- ions and the lower threshold voltage from applying thermal energy. Based on the effects of elevated ambient temperature and low humidity as shown in figures 1–3, it is suggested that the higher temperature is needed to fabricate nanostructures with a high aspect ratio and to fabricate protruded nanopatterns at high lithographic speeds.

For the application of pattern fabrication on metal thin films using AFM lithography, protruded nanostructures of Ta_2O_5 with heights of about 1 nm, full widths of about 100 nm and a line and space of 250 nm were fabricated. After protruded metal oxide structures were entirely removed by etching, Ta

nanopatterns had a line width of about 100 nm and a depth of about 1–2 nm as shown in figure 4. Carbon fluoride (C_4F_8) gas was utilized for etching Ta_2O_5 [19] because it has a high selectivity between Ta and Ta_2O_5 . The volatile by-product TaF_5 , formed by the chemical reaction between C_4F_8 and Ta_2O_5 due to the relatively low boiling point (229.5 °C), successfully removes protruded Ta_2O_5 [20]. However, the roughness of the Ta nanopatterns increased in the range of 0.1 to 0.4 nm because TaC, which has a very high boiling point (5500 °C) [20], was adsorbed on the Ta surface. Ta nanopatterns with high angle slope of about 80° are observed despite using a Pt-coated cantilever tip with a curvature radius of about 35 nm.

We have investigated the effect of applied thermal energy on nanostructures in the AFM lithography process and fabrication of Ta nanopatterns by dry etching. To fabricate

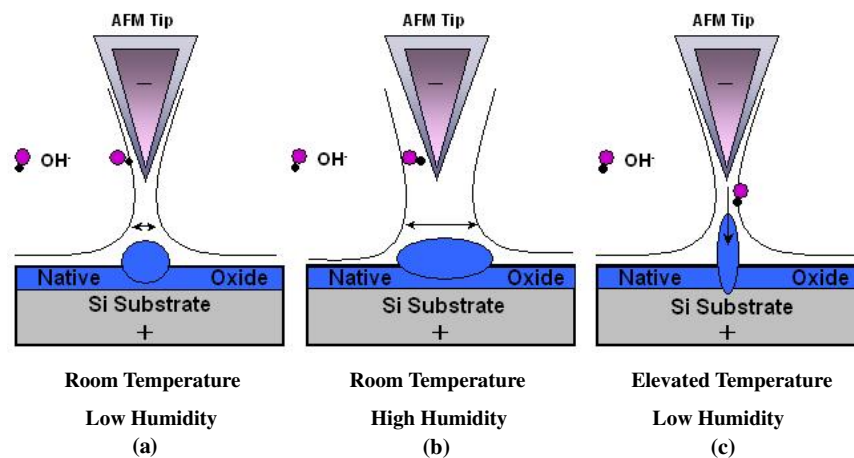


Figure 2. Schematic representation of the water meniscus between a tip and a substrate as a function of the variation of temperature and humidity during AFM lithography.

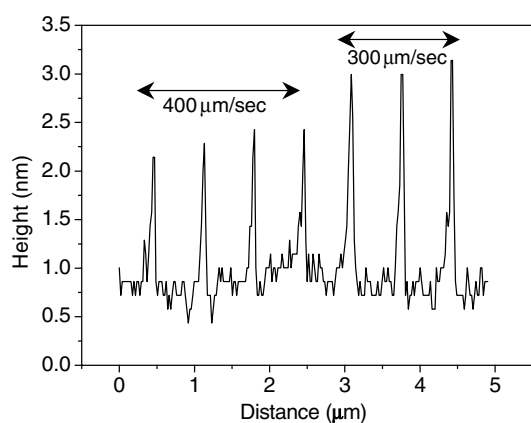
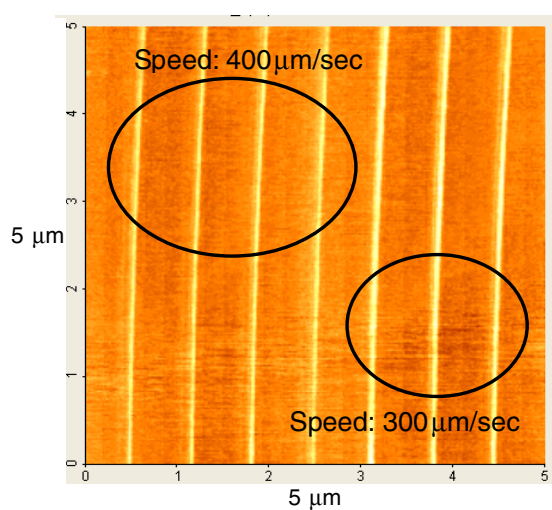


Figure 3. AFM image of protruded nanostructures fabricated at high lithographic speeds ($300\text{--}400\ \mu\text{m s}^{-1}$, from right to left) under an elevated temperature of $31\ ^\circ\text{C}$ and low humidity (30%). The height of the nanostructures is 2.5 and 1.7 nm and the FWHM is 60 and 38 nm, respectively.

nanostructures at high lithographic speeds with a high aspect ratio, higher temperature by an enhanced thermal energy which can lower the threshold voltage and promote growth,

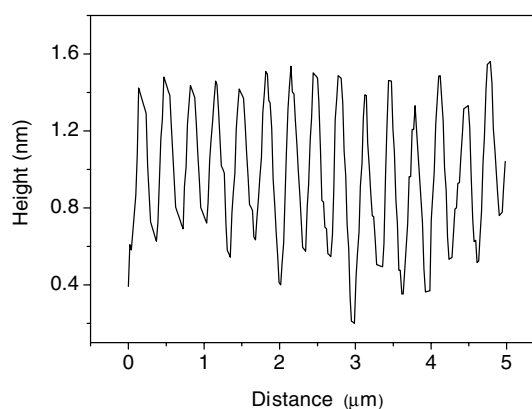
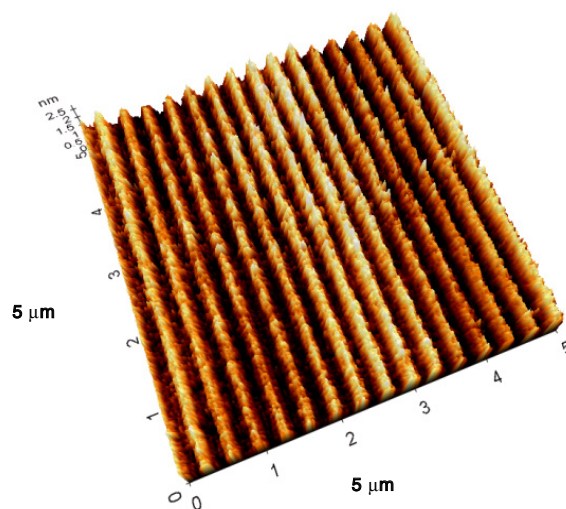


Figure 4. AFM image of Ta nanopatterns after selective dry etching. Etched nanopatterns have a high angle slope over about 80° .

is strongly needed. Based on these observations, we obtained oxidized nanostructures with a high aspect ratio of 0.15–0.21 and protruded nanostructures of about 1.7 nm in line height and about 38 nm in line width at the high speed of $400\ \mu\text{m s}^{-1}$

under the elevated temperature. Moreover, after etching Ta₂O₅ nanostructures fabricated by AFM lithography, we obtained Ta nanopatterns with feature sizes in the range of 100 nm.

Acknowledgment

This work was supported by the National Program for Tera-Level Nanodevices of the Ministry of Science and Technology as one of the 21st Century Frontier Programs.

References

- [1] Wang Y, Yun W and Jacobsen C 2003 *Nature* **424** 50
- [2] Solak H H, He D, Li W, Singh-Gasson S, Sohn B H, Yang X M, Nealey P and Cerrina F 1999 *Appl. Phys. Lett.* **75** 2328
- [3] Bartels R A, Paul A, Green H, Kapteyn H C, Murnane M M, Backus S, Christov I P, Liu Y, Attwood D and Jacobsen C 2002 *Science* **297** 376
- [4] Lercel M J, Rooks M, Tiberio R C, Sheen C W, Parikh A N, Allara D L and Craighead H G 1995 *J. Vac. Sci. Technol. B* **13** 1139
- [5] Chen Y, Ohlberg D A A, Li X, Stewart D R, Stanley Williams R, Jeppesen J O, Nielsen K A, Fraser Stoddart J, Olynick D L and Anderson E 2003 *Appl. Phys. Lett.* **82** 1610
- [6] Lyuksyutov S F, Vaia R A, Paramonov P B, Juhl S, Waterhouse L, Ralich R M, Sigalov G and Sancaktar E 2003 *Nat. Mater.* **2** 468
- [7] Sugimura H and Nakagiri N 1996 *J. Vac. Sci. Technol. A* **14** 1223
- [8] Lee W B, Kim E R and Lee H 2002 *Langmuir* **18** 8375
- [9] Lyuksyutov S F, Paramonov P B, Dolog I and Ralich R M 2003 *Nanotechnology* **14** 716
- [10] Demers L M, Ginger D S, Park S-J, Li Z, Chung S-W and Mirkin C A 2002 *Science* **296** 1836
- [11] Calleja M and Garcia R 2000 *Appl. Phys. Lett.* **76** 3427
- [12] Rosolen G C, Hoole A C F, Welland M E and Broers A N 1993 *Appl. Phys. Lett.* **63** 2435
- [13] Dagata J A, Inoue T, Itoh J, Matsumoto K and Yokoyama H 1998 *J. Appl. Phys.* **84** 6891
- [14] Tello M and Garcia R 2003 *Appl. Phys. Lett.* **83** 2339
- [15] Avouris Ph, Martel R, Hertel T and Sandstrom R 1998 *Appl. Phys. A* **66** S659
- [16] Mangat P J S *et al* 1999 *J. Vac. Sci. Technol. B* **17** 3029
- [17] Racette K, Brooks C, Richard Guarnieri C and Hendy D 2000 *J. Vac. Sci. Technol. A* **18** 1119
- [18] Wolf S and Tauber R N 2000 *Silicon Processing for the VLSI Era*. 2nd edn, vol 1 *Process of Technology* (California: Lattice Press) p 151
- [19] Ibbotson D E, Mucha J A, Flamm D L and Cook J M 1985 *Appl. Phys. Lett.* **46** 794
- [20] Weast R C and Astle M J 1982 *CRC Handbook of Chemistry and Physics* 63rd edn (Boca Raton, FL: CRC Press) p B-154